MiR-30c-1-3p Targets Matrix Metalloproteinase 9 Involved into the Rupture of Abdominal Aortic Aneurysms

Lin Yang
General Hospital of Northern Theatre command
Hong-gang Sui
General Hospital of Northern Theatre command
Meng-meng Wang
General Hospital of Northern Theatre command
Jia-yin Li
General Hospital of Northern Theatre command
Xiao-feng He
General Hospital of Northern Theatre command
Jing-yuan Li
General Hospital of Northern Theatre command
Xiaozeng Wang (wxiaozeng@163.com)
General Hospital of Northern Theater Command https://orcid.org/0000-0003-1979-0287

Research Article

Keywords: abdominal aortic aneurysm, microRNA, miR-30c-1-3p, matrix metalloproteinase 9

Posted Date: November 30th, 2021

DOI: https://doi.org/10.21203/rs.3.rs-1043662/v1

Abstract

Abdominal aortic aneurysm (AAA) can be fatal if ruptured, but there is no predictive biomarker. Our aim was to evaluate the prognostic potential of microRNAs (miRNAs/miRs) in an AAA mouse model and patients with unruptured AAA (URAAA) and ruptured AAA (RAAA). Among the 64 miRNAs differentially expressed in mice with AAA compared to control, miR-30c-1-3p, miR-432-3p, miR-3154, and miR-379-5p had high homology with human miRNAs. MiR-30c-1-3p plasma levels were significantly lower in patients with RAAA than in those with URAAA or control and tended to negatively correlate with the maximum aortic diameter (r = -0.3153, P = 0.06109). Mir-30c-1-3p targeted matrix metalloproteinase (*MMP)-9* mRNA through the coding region and downregulated its expression *in vitro*. MMP-9 plasma concentrations were significantly higher in the RAAA group than in the URAAA group (P < 0.001) and were negatively associated with miR-30c-1-3p levels (r = -0.3671, P = 0.01981) and positively – with the maximal aortic diameter (r = 0.6251, P < 0.0001). The optimal cutoff values for MMP-9 expression and the maximal aortic diameter were 461.08 ng/ml and 55.95 mm, with areas under the curve of 0.816 and 0.844, respectively. Our results indicate that plasma levels of mir-30c-1-3p and MMP-9 may be candidate biomarkers of AAA progression.

Key Message

1. This is the first study to report that downregulation of miR-30c-1-3p expression and upregulation of its potential target MMP-9 can acceleration of AAA development.
2. Its could be a potential biomarker of AAA development and the risk of AAA rupture.

Introduction

Abdominal aortic aneurysm (AAA) is caused by degeneration of the arterial wall resulting in continuous dilation of the abdominal aorta, whose diameter can exceed that of the normal aorta by more than 1.5 times. Ruptured AAAs (RAAAs) are associated with a very high overall mortality rate – over 90%[1] and there is an urgent need for reliable biomarkers that can be easily detected in circulation to facilitate systemic screening of the population at risk[2]. However, AAA is a multifactorial condition that could be promoted by genetic and environmental factors, changes in hemodynamics, inflammatory response to pathogenic microorganisms, apoptosis of smooth muscle cells, and inflammation of perivascular adipose tissue. Despite the recent improvements in the diagnostics and therapy of AAA, the associated morbidity and mortality remain high[2, 3]. The molecular mechanisms underlying AAA development are not fully understood and specific biomarkers to predict the initiation and progression of AAA are unknown.

MicroRNAs (miRNAs) are small noncoding RNAs with a length of 18-24 nucleotides, which are known as post-transcriptional regulators of gene expression. MiRNAs bind to complementary sites in 3'-untranslated regions (3'-UTRs) of specific mRNA targets, inhibiting their translation or inducing degradation[4]. A single miRNA can alter the expression of multiple genes and exert effects on several

physiological mechanisms. MiRNAs are very stable in the extracellular space and can be found in body fluids such as blood[5]. Many studies have explored the relationship between miRNAs and AAA[6–8] and several thousands of human miRNA sequences with unique expression in different tissues at specific stages of AAA development are expected to serve as new diagnostic biomarkers and therapeutic targets. However, published studies often involve too few participants and yield sample types and results are contradictory or inconsistent. In this study, we constructed an AAA mouse model under the pathological conditions of both high fat and hypertension, and further adopted miRNA array analysis to determine the differentiated miRNAs that are highly homologous and consistent with AAA diagnosis.We selected relevant genes for verification in patient serum, and examined the correlation between plasma miRNA levels and AAA severity.

Results

Evaluation of differential expression of miRNAs in AAA tissues in ApoE-/- mouse fed with western diet

To mimic the human AAA injury, an AAA model was created in apolipoprotein E knockout (*ApoE*-/-) mice fed with western diet and infusing angiotensin II (AngII) (1 μg/kg/min) for 4 weeks; The control group was infused with saline and chow diet. The protuberance of the abdominal aorta in AngII-infused mice was more formation and rupture of AAA than in control, indicating successful establishment of the AAA model (Figure 1A). AAA formation and mortality rates in the AAA group were 60% and 10%, respectively (Figure 1B, C). Compared to the control group, the average blood pressure was elevated in the AAA group (P=0.088) (Figure 1D), whereas the body weight slightly reduced (P=0.116) (Figure 1E). The levels of total cholesterol (TC) (31.60±6.99 *vs.* 17.15±3.53, P<0.01) and triglyceride (TG) (3.96±0.72 *vs.* 2.39±0.79, P<0.01) were significantly higher in the AAA group than in the control group (Figure 1F–G). Furthermore, miRNA microarray analysis revealed the differential expression of 64 miRNAs in the aorta of AAA mice compared to control mice (Figure 2A). Among them, we obtained four miRNAs with high homology to human miRNAs for further analysis (Figure 2B).

Identification of plasma miRNAs differentially expressed in patients with AAA

Supplemental Table 1 shows clinicopathological characteristics of 20 patients with URAAA, 20 patients with RAAA, and 19 patients with coronary artery disease (CAD) used as a control group. All participants were men, and there were no significant differences in age, diabetes mellitus, hypertension, or smoking habits between the control and AAA (URAAA and RAAA) groups. Statistically significant difference was observed between patients with URAAA and RAAA in the maximum diameter of aortic aneurysms (4.78 ± 0.55 cm *vs*. 6.34 ± 1.33 cm, P < 0.001) (Supplemental Table 1).

Plasma of patients with RAAA and URAAA and the control group was analyzed four miRNAs expression by quantitative (q)RT-PCR. The results indicated that plasma levels of hsa-miR-30c-1-3p were significantly lower (P=0.0013), whereas those of hsa-miR-432-3p were significantly higher in the RAAA group than in the control and URAAA groups (P=0.0106) (Figure 3A, B). The expression of miR-3154 was the highest in

the URAAA group, followed by the RAAA group and control group and that of miR-379-5p was the highest in the URAAA group, followed by the control group and URAAA group (Figure 3C, D).

Correlation between the maximal aortic diameter and miRNA levels

Bivariate correlation analysis showed that plasma levels of miR-30c-1-3p in patients with AAA tended to be negatively correlated with the maximal aortic diameter (Pearson correlation coefficient r = -0.3153, P = 0.06109) (Figure 4A). There was no correlation between plasma levels of mir-432-3p (Pearson correlation coefficient r = 0.01851, P = 0.4987), mir-3154 (Pearson correlation coefficient r = 0.04215, P = 0.4293), and mir-379-5p (Pearson correlation coefficient r = 0.1055, P = 0.1508) and the maximal aortic diameter in patients with AAA (Figure 4B–D).

Prediction of miRNA target genes and their functional annotation

To disclose potential physiological mechanisms regulated by differentially expressed miR-30c-1-3p, its target genes were predicted using miRWalk, miRanda, RNA22, and Targetscan, and the common targets identified by the four databases were revealed by the Venn diagram (Figure 5A). Next, the target genes were functionally annotated using Gene Ontology (GO) and Kyoto Encyclopedia of Genes and Genomes (KEGG) databases. The target genes of miR-30c-1-3p were distributed according to GO biological processes, cell composition, and molecular function (Figure 5B). KEGG pathway analysis revealed the top three enriched pathways for miR-30c-1-3p targets, which were axon guidance, MAPK signaling pathway, and thyroid hormone signaling pathway (Figure 5B).

Inhibition of MMP-9 expression by miR-30c-1-3p in vitro

Prediction analysis identified *MMP-9* as a potential target gene of mir-30c-1-3p. To elucidate whether miR-30c-1-3p directly regulated MMP-9 expression, we induced or reduced miR-30c-1-3p levels in RAW264.7 cells using a miR-30c-1-3p mimic or inhibitor, respectively. Western blot analysis showed that miR-30c-1-3p overexpression decreased the expression of MMP-9 in RAW264.7 cells, whereas its inhibition had the opposite effect (Figure 6A, B).

MiR-30c-1-3p inhibited MMP-9 expression through binding to its coding sequence and not to 3'-UTR

To further examine the inhibitory effect of miR-30c-1-3p on MMP-9 expression, we transfected HEK293 cells with a reporter vector for the 3'-UTR of *MMP-9*, which contained miR-30c-1-3p-targeted base pairs (Figure 6C, D). However, the dual-luciferase reporter assay did not reveal significant differences in luciferase activity between cells co-transfected with 3'-UTR and miR-30c-1-3p mimic or scrambled control (Figure 6E), indicating that miR-30c-1-3p did not regulate *MMP-9* expression through its 3'-UTR. Interestingly, we found another conserved miR-30c-1-3p target site in the *MMP-9* coding sequence (Figure 6F, G), and it appeared to be the region through which miR-30c-1-3p regulated *MMP-9* expression according to the reporter assay (Figure 6H). To validate this result, we mutated the *MMP-9* site targeted by miR-30c-1-3p in the coding sequence and co-transfected HEK293 cells with the mutated vector and miR-30c-1-3p or scrambled control. There was no significant difference in MMP-9 expression between the

cells transfected with miR-30c-1-3p or control miR (Figure 6H), confirming that miR-30c-1-3p inhibited *MMP-9* expression through binding to its coding sequence.

MMP-9 expression was correlated with miR-30c-1-3p levels and the maximal aortic diameter

Analysis of patients' samples revealed that MMP-9 plasma concentration was increased in the URAAA and RAAA groups compared to control ($P < 0.001$) and in the RAAA group compared to the URAAA group ($P < 0.001$) (Figure 7A, Supplemental Table 2). Bivariate correlation analysis indicated that MMP-9 levels in plasma of patients with AAA was positively correlated with the maximal aortic diameter ($r = 0.6251$, $P < 0.0001$; Figure 7B) and negatively – with miR-30c-1-3p expression ($r = -0.3671$, $P = 0.01981$; Figure 7C).

MMP-9 expression and the maximal aortic diameter could predict the risk of AAA rupture

Receiver operating characteristic (ROC) curve analysis demonstrated that MMP-9 expression and the maximum aortic diameter could be used to distinguish patients with URAAA from those with RAAA (Figure 8). The optimal cutoff values for MMP-9 expression and the maximal aortic diameter were 461.08 ng/ml and 55.95 mm with areas under the curve of 0.816 and 0.844, respectively.

Discussion

In the present study, a modified AAA model was used, that is, AAA group mice were fed a western diet for 4 weeks before Ang II injection and continued on the same diet afterwards. The results showed that AAA formation and mortality rates in the AAA group were 60% and 10%, respectively. In previous study, AAA occurred in 33% of mice in the group infused with 1,000 ng/min/kg of Ang II[9]. Compared with that, the modified AAA model fed with Western diet in this study can effectively improve the formation rate of AAA, and it is more similar to clinical.

Accumulating evidence indicates that the deregulation of miRNA expression can have profound effects on extracellular matrix remodeling, cell cycle, aging, and inflammation[10] and is associated with many diseases, including cancer, cardiovascular diseases, and neurological disorders[11–13]. MiRNAs are distinguished by high extracellular stability and can be detected in blood and other body fluids; therefore, circulating miRNAs share many characteristics essential for biomarkers, such as sensitivity, specificity, and a long half-life in the sample, as well as rapid and cost-effective laboratory detection.

In this study, we showed that the miRNA expression profile in plasma of patients with AAA differed from that of patients with CAD and that the levels of circulating miR-30c-1-3p was different in patients with URAAA and RAAA, suggesting that these miRNAs could be novel candidate biomarkers for AAA progression. Among the four identified miRNAs, miR-30c-1-3p plasma levels were significantly lower in patients with RAAA than in those with URAA. Furthermore, there was no previous study on mir30c-1-3p related to AAA. In search for miR-30c-1-3p targets, we identified MMP-9, which showed negative correlation with miR-30c-1-3p levels and positive correlation with the maximal aortic diameter. According to ROC curves for RAAA prediction, MMP-9 expression or the maximal aortic diameter was greater than

461.08 ng/ml or 55.95 mm may indicate the risk of AAA rupture, respectively. These results implicate the miR-30c-1-3p/MMP-9 axis in AAA progression to rupture.

It has been shown that miRNA-30c attenuates hyperlipidemia, hypercholesterolemia, and atherosclerosis in mice[14, 15] and plays an important role in angiogenesis[16]. Our KEGG pathway analysis revealed that miR-30c-1-3p targets were enriched in the axonal guidance, thyroid hormone signaling, and MAPK signaling pathways. Indeed, previous studies indicate that the MAPK pathway is the key biochemical mechanism involved in AAA[17]. Furthermore, MMP-9, one of the main mir-30c-1-3p targets, has been reported to contribute to the rupture of AAAs[18], whereas MMP-9 plasma concentrations are positively correlated with the AAA growth rate[19] and AAA rupture[20, 21]. These findings are consistent with our results that MMP-9 levels in patients with RAAA were significantly higher than those in patients with URAAA and that MMP-9 concentration exceeding 461.08 ng/ml may indicate the risk of AAA rupture.

As a rule, miRNAs bind to complementary sites in 3'-UTRs of specific mRNA targets[22] and through this, exert their effects on diverse cellular processes, including cell proliferation, differentiation, and apoptosis[23, 24]. An interesting finding of our study is that miR-30c-1-3p regulated MMP-9 expression through binding to its coding region rather than 3'-UTR, which is, to the best of our knowledge, shown for the first time.

In conclusion, our results suggest that the downregulation of miR-30c-1-3p expression can result in the upregulation of its potential target MMP-9, increase in the aorta diameter, and acceleration of AAA development. A change in miR-30c-1-3p serum levels may indicate the stage of AAA progression and serve as a potential biomarker of AAA development and the risk of AAA rupture.

Methods

Ethics

Both human serum samples and animal studies were approved by the Clinical Research Committee and the Institutional Animal Care and Use Committee of General Hospital of Northern Theater Command respectively. All human studies adhered to the guidelines of the Declaration of Helsinki. All participants in the experiment provided informed consent. All animal experiments complied with the Guide for the Care and Use of Laboratory Animals published by the United States National Institutes of Health.

Animal model and samples

We used 6–8 week-old male *ApoE*-/- mice (weight 20–25 g) purchased from Jackson laboratories (Bar Harbor, ME, USA). Mice were infused with Ang II (Sigma Chemical Co; # a-9295, USA) at 1 μg/kg/min (the dose was based on a previous study[9]) for 4 weeks using a micro-osmotic pump (model 1004, ALZET Osmotic Pumps, Cupertino, CA, USA). AAA group mice were fed a western diet for 4 weeks before Ang II injection and continued on the same diet afterwards. Control group mice were fed a chow diet and infused with saline. The level of abdominal aorta from the left renal artery to the suprarenal area was

analyzed by echocardiography. Images of the whole aorta were obtained by scanning the long and short aorta axes. Each mouse was scanned three times by an investigator blinded to the nature of treatment. Blood pressure was measured by the tail-cuff method using a Softron BP2010A Blood Pressure Meter (Softron Beijing Biotechnology Co., Ltd, Beijing, China). The tail was fixed to the sphygmomanometer, and sensors were used to record blood pressure indirectly. Blood pressure was measured at least three times in each mouse at 0, 7, 14, and 28 days. Mice that died during the experiment were dissected, and RAAAs were detected based on dilated perivascular blood clots or abdominal bleeding; these mice were included in the assessment of the tumor formation rate and risk of rupture. The surviving mice were euthanized under anesthesia at day 28, and the aorta (from the ascending aorta to the iliac artery) was dissected out. The AAA specimens were frozen at -80 ℃, transferred into centrifuge tubes, sealed on dry ice, and mailed to BioMiao Biological Technology Co., Ltd. (Beijing, China) for microarray analysis.

Microarray analysis

miRNA expression in mouse aortas was analyzed by BioMiao Biological Technology Co., Ltd (Beijing, China) using the Agilent Mouse miRNA Microarray Kit, Release 21.0, 8 × 60 K (Design ID:070155; Agilent Technologies, Santa Clara, CA, USA), which contained 1902 probes for mature miRNA.

Patient cohorts

In total, 59 patients were included in the study: 20 with RAAA, 20 with URAAA, and 19 with CAD (control group). To assess the maximal aortic diameter and the presence of an entry tear, all patients underwent computed tomographic angiography (CTA) during hospitalization, as previously described[25]. CTA was carried out using a Siemens Somatom Sensation 64 CT Scanner after administration of intravenous boluses containing 80–150 mL of nonionic contrast medium; three measurements were performed and the mean values were calculated.

miRNA isolation from blood samples and qRT-PCR

Peripheral venous blood was collected from patients into EDTA-containing tubes and centrifuged at 3000 × *g* for 10 min at 4 ℃, and plasma was stored at -80 ℃. Total RNA was extracted from 200 microliter plasma samples by using the miRNeasy Serum/Plasma Kit (Qiagen, Hilden, Germany) and cDNA was synthesized using a reverse transcription kit (RiboBio, Guangzhou, China) according to the manufacturer's instructions. After equal volume dilution of cDNA (20 microliters of DNase/RNase-Free Deionized water was added to 20 microliters of cDNA), the expression levels of miR-30c-1-3p, miR-432-3p, miR-3154, and miR-379-5p were evaluated by Quantitative real-time Polymerase Chain Reaction (qRT-PCR) using specific primers (Supplemental Table 3) and the miDETECT A TrackTM miRNA qRT-PCR Kit (RiboBio) following the manufacturer’s protocol; reactions were performed on a CFX96 Touch™ Real-Time PCR Detection System (Hercules, California, USA). Each reaction was performed in triplicate, the relative expression level of miRNAs were calculated based on cycle threshold (Ct) values through formula 2-ΔCt, which ΔCt value is the Ct value of miRNAs in each patient of URAAA/RAAA group minus the average Ct value of miRNAs in the control group.

Western blot analysis

Cells and tissues were homogenized using a RIPA buffer (Thermo Fisher Scientific, Glen Burnie, MD) supplemented with protease and phosphatase inhibitors. The total protein was estimated using the BCA protein assay reagent kit (Thermo Fisher Scientific). Briefly, 40 µg total protein was loaded and detected with antibodies against MMP9 (Cell Signaling Technology, Danvers, MA, US), glyceraldehyde-3-phosphate dehydrogenase (GAPDH) (Cell Signaling Technology).

Functional annotation of differentially expressed miRNAs

The target genes of differentially expressed miRNAs were predicted using miRWalk, miRanda, RNA22, and Targetscan)http://zmf.umm.uni-heidelberg.de/apps/zmf/mirwalk2/)and analyzed based on GO terms enrichment in three functional categories: molecular function, cellular component, and biological process[26]. KEGG was used for the functional classification of miRNAs according to the relevant biological pathways and for analysis of their relative enrichment.

Cell culture and transfections

We obtained RAW 264.7 cells and human embryonic kidney HEK293 cells lines from the Chinese Academy of Sciences Cell Bank. Mouse macrophage RAW 264.7 cells and HEK293 cells were maintained in Dulbecco's modified Eagle's medium (DMEM; Life Technologies Corporation, Carlsbad, CA, USA) supplemented with 10% fetal bovine serum (Life Technologies) at 37°C in a humidified atmosphere of 5% CO2. RAW 264.7 cells were transfected with a miRNA mimic (100 nM), miRNA inhibitor (100 nM), or their controls (RiboBio, Guangzhou, China) using Lipofectamine RNAiMAX (Invitrogen, Carlsbad, CA, USA) following the manufacturer's protocol, collected after 48 h, and analyzed for MMP-9 expression by western blotting. HEK293 cells were used for the dual-luciferase reporter assay described below.

Dual-luciferase reporter assay

PmirGLO Dual-Luciferase miRNA Target Expression plasmids containing the *MMP-9* 3'-UTR or coding sequence were synthesized by GENEWIZ (Suzhou, China) and amplified it in E. coli. The plasmids were extracted using the Wizard® Plus SV Minipreps DNA Purification System (Promega, Madison, WI, USA) according to the manufacturer's instructions.

HEK293 cells were co-transfected with 200 ng of pmirGLO Dual Luciferase plasmids, and miR-30c-1-3p mimic (100 nM) or mimic control (100 nM) using X-tremeGENE HP DNA Transfection Reagent (Sigma, St. Louis, MO, USA) .

Luciferase activity was analyzed by the Dual-Luciferase Reporter Assay System (Promega) following the manufacturer's protocol. Transfection efficiency was normalized by *Renilla* luciferase activity.

Biochemical analysis

Serum samples were analyzed for TC (Nanjing Jiancheng Bioengineering Institute, Nanjing, China), TG (Nanjing Jiancheng Bioengineering Institute) by using the total cholesterol and triglyceride quantification kit according to the manufacturers' instructions.

Measurement of MMP-9 plasma concentration

Plasma levels of MMP-9 were determined by enzyme linked immunosorbent assay (ELISA) using a human MMP-9 ELISA kit (no. ab246539, Abcam, UK) according to the manufacturer's instructions.

Statistical analysis

Continuous variables were reported as the mean ± standard deviation (SD) or medians and interquartile ranges (25th or 75th percentiles) and compared by unpaired Student's *t*-test, one-way ANOVA, or Mann-Whitney U test. Categorical variables were expressed as percentages and compared by chi-square test or Fisher's exact tests. Pearson correlation coefficient (*r*) was used for bivariate normally distributed data. The prediction potential of MMP-9 expression or the maximal aortic diameter was evaluated by ROC curve analysis. The optimal cutoff level was calculated by the Youden index (sensitivity + specificity - 1). GraphPad Prism 8.0 (GraphPad, La Jolla, CA, USA) was used for graphical data presentation. SPSS version 22.0 was used for statistical analysis (IBM, Armonk, New York, NY, USA). The level of significance was set at $P < 0.05$.

Declarations

Ethics approval

Both human serum samples and animal studies were approved by the Clinical Research Committee and the Institutional Animal Care and Use Committee of General Hospital of Northern Theater Command respectively, File No: [2021] Ethical Review [Clinical Research] No. 002).

Consent to participate

Not applicable.

Consent for publication

Not applicable.

Availability of data and materials

Data and materials will be shared upon request

Competing Interests

The authors declare no competing interests.

Funding Information

This work was supported by Department of Science and Technology of Liaoning Province (2020020096-JH2/103).

Authors' contributions

All authors confirm they contributed to the intellectual content of this article including conception and design.W.X. and Y.L. conceived the project and designed the study. S.H.and W.M. conducted Quantitative real-time Polymerase Chain Reaction. Y.L. and L.J. conducted western blotting and site-directed mmutagenesis, H.X. and L.J. checked the manuscript. Y.L. wrote the manuscript. All authors read and approved the final paper.

Acknowledgments

We are grateful to the subjects who participated in the study and for the physician assistance in this study.

References

1.Duncan R, Essat M, Jones G et al (2017) Systematic review and qualitative evidence synthesis of patient-reported outcome measures for abdominal aortic aneurysm. Br J Surg 104: 317-327.

2.Nordon IM, Hinchliffe RJ, Loftus IM et al (2011) Pathophysiology and epidemiology of abdominal aortic aneurysms. Nat Rev Cardiol 8: 92-102.

3.Lee MJ, Daniels SL, Drake TM et al (2016) Risk factors for ischaemic colitis after surgery for abdominal aortic aneurysm: a systematic review and observational meta-analysis. Int J Colorectal Dis 31: 1273-1281.

4. Bartel DP (2004) MicroRNAs: genomics, biogenesis, mechanism, and function. Cell 116:281–97.

5. Ambros V, microRNAs: tiny regulators with great potential. [J]. Cell, 2001, 107(7): 823-826.

6. Kin K, Miyagawa S, Fukushima S et al (2012) Tissue- and plasma-specific MicroRNA signatures for atherosclerotic abdominal aortic aneurysm. J Am Heart Assoc 1: e000745.

7. Borek A, Drzymała F, Botor M et al (2019) Roles of microRNAs in abdominal aortic aneurysm pathogenesis and the possibility of their use as biomarkers. Kardiochir Torakochirurgia Pol 16:124-127.

8. Stather PW, Sylvius N, Sidloff DA (2015) Identification of microRNAs associated with abdominal aortic aneurysms and peripheral arterial disease. Br J Surg 102:755-766.

9.Daugherty A, Manning MW, Cassis LA (2000) Angiotensin II promotes atherosclerotic lesions and aneurysms in apolipoprotein E-deficient mice. J Clin Invest 105:1605-1612.

10. Borek A, Drzymała F, Botor M et al (2019) Roles of microRNAs in abdominal aortic aneurysm pathogenesis and the possibility of their use as biomarkers. Kardiochir Torakochirurgia Pol 16:124-127.

11. Friedman RC, Farh KK, Burge CB et al (2009) Most mammalian mRNAs are conserved targets of microRNAs. Genome Res 19: 92-105.

12. Thomas M, Lieberman J, Lal A (2010) Desperately seeking microRNA targets. Nat Struct Mol Biol 17: 1169-1174.

13. Salomão KB, Pezuk JA, de Souza GR et al (2019) MicroRNA dysregulation interplay with childhood abdominal tumors. Cancer Metastasis Rev 38: 783-811.

14. Soh J, Iqbal J, Queiroz J et al (2013) MicroRNA-30c reduces hyperlipidemia and atherosclerosis in mice by decreasing lipid synthesis and lipoprotein secretion. Nat Med 19:892–900.

15. Irani S, Pan X, Peck BCE et al (2016) MicroRNA-30c mimic mitigates hypercholesterolemia and atherosclerosis in mice. J Biol Chem 291:18397–18409.

16. Bridge G, Monteiro R, Henderson S et al (2012) The microRNA-30 family targetsDLL4to modulate endothelial cell behavior during angiogenesis. Blood 120:5063-5072.

17. Piacentini L, Chiesa M, Colombo GI (2020) Gene Regulatory Network Analysis of Perivascular Adipose Tissue of Abdominal Aortic Aneurysm Identifies Master Regulators of Key Pathogenetic Pathways. Biomedicines 8:288.

18. Wilson WR, Anderton M, Schwalbe EC et al (2006) Matrix metalloproteinase-8 and -9 are increased at the site of abdominal aortic aneurysm rupture. Circulation 113: 438-445.

19. Speelman L, Hellenthal FA, Pulinx B et al (2010) The influence of wall stress on AAA growth and biomarkers. Eur J Vasc Endovasc Surg 39: 410-416.

20. Petersen E, Gineitis A, Wågberg F et al (2000) Activity of matrix metalloproteinase-2 and -9 in abdominal aortic aneurysms. Relation to size and rupture. Eur J Vasc Endovasc Surg 20:457-461.

21. Petersen E, Wågberg F, Angquist KA (2002) Proteolysis of the abdominal aortic aneurysm wall and the association with rupture. Eur J Vasc Endovasc Surg 23: 153-157.

22. Farh KK, Grimson A, Jan C et al (2005) The widespread impact of mammalian MicroRNAs on mRNA repression and evolution. Science 310: 1817-1821.

23. Tomasetti M, Gaetani S, Monaco F et al (2019) Epigenetic Regulation of miRNA Expression in Malignant Mesothelioma: miRNAs as Biomarkers of Early Diagnosis and Therapy. Front Oncol 9: 1293.

24.Cacheux J, Bancaud A, Thierry L et al (2019) Technological Challenges and Future Issues for the Detection of Circulating MicroRNAs in Patients with Cancer. Front Chem 7: 815.

25. Lovy AJ, Rosenblum JK, Levsky JM et al (2013) Acute aortic syndromes: a second look at dual-phase CT. AJR Am J Roentgenol 200: 805-811.

26. Ashburner M, Ball CA, Blake JA et al (2000) Gene ontology: tool for the unification of biology. Nat Genet 25:25-29.

Figures

Figure 1

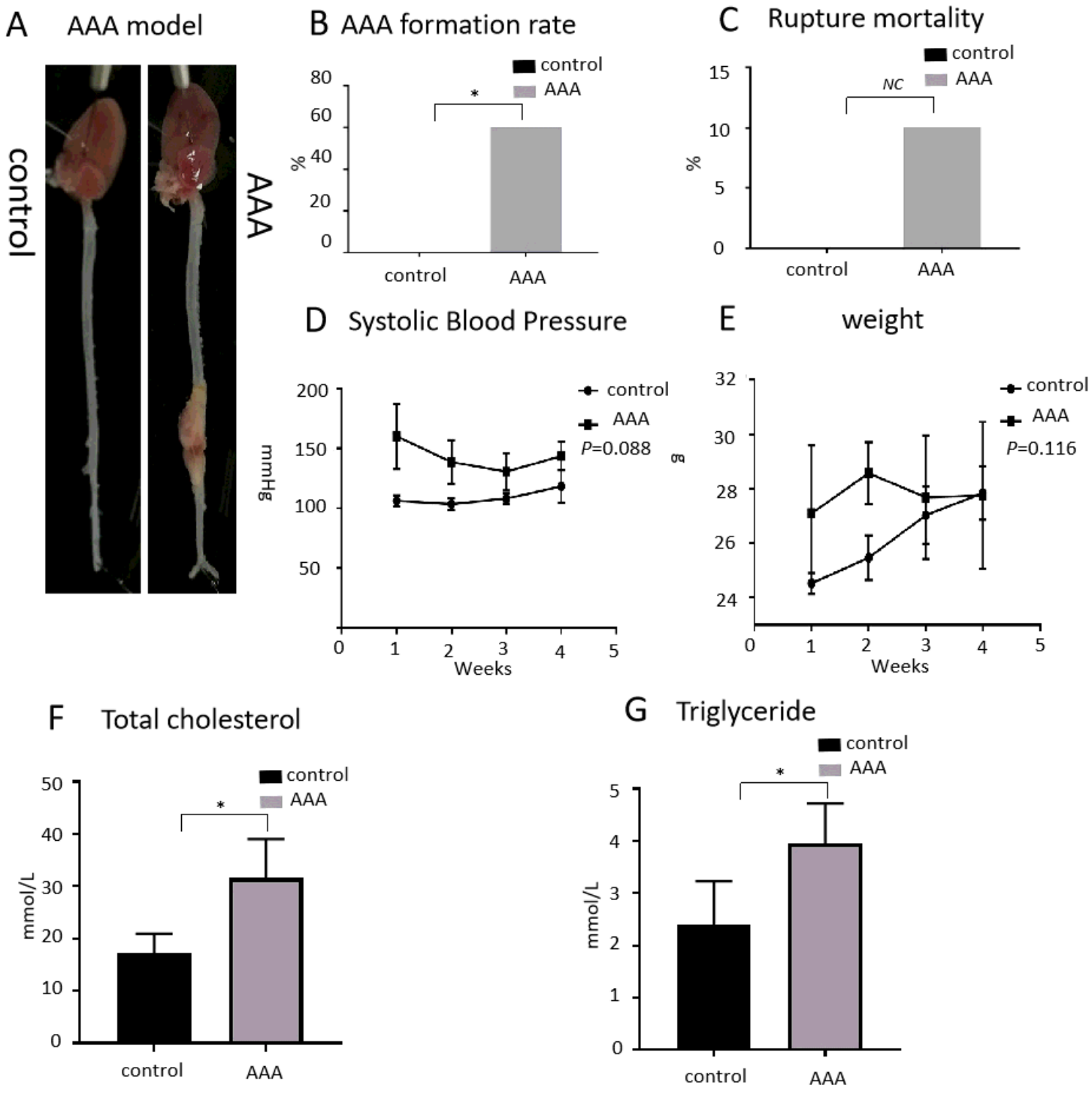

Figure 1

The protuberance of the abdominal aorta in AngII-infused mice was more formation and rupture of AAA than in control, indicating successful establishment of the AAA model (Figure 1A). AAA formation and mortality rates in the AAA group were 60% and 10%, respectively (Figure 1B, C). Compared to the control group, the average blood pressure was elevated in the AAA group (P=0.088) (Figure 1D), whereas the body weight slightly reduced (P=0.116) (Figure 1E). The levels of total cholesterol (TC) (31.60±6.99 vs.

17.15±3.53, P<0.01) and triglyceride (TG) (3.96±0.72 vs. 2.39±0.79, P<0.01) were significantly higher in the AAA group than in the control group (Figure 1F–G).

Figure 2

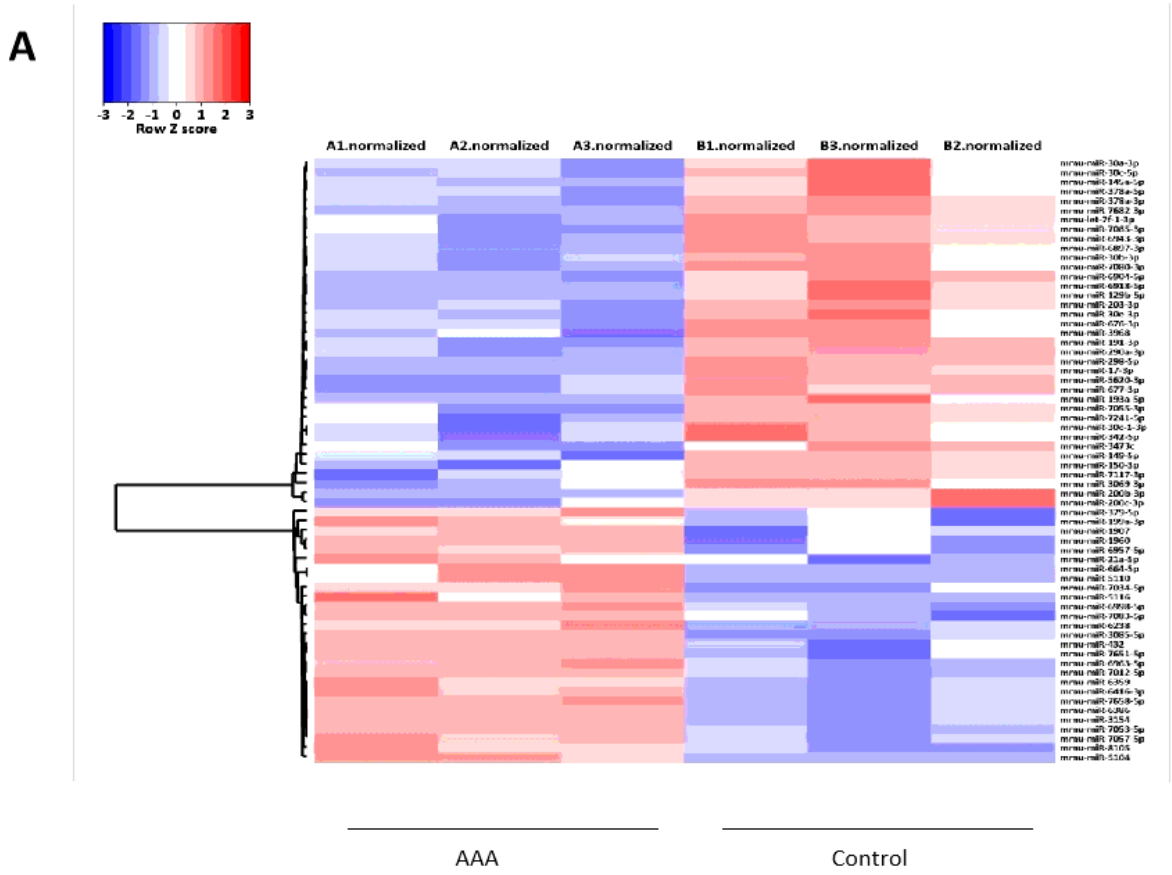

Figure 2

Furthermore, miRNA microarray analysis revealed the differential expression of 64 miRNAs in the aorta of AAA mice compared to control mice (Figure 2A). Among them, we obtained four miRNAs with high homology to human miRNAs for further analysis (Figure 2B).

Figure 3

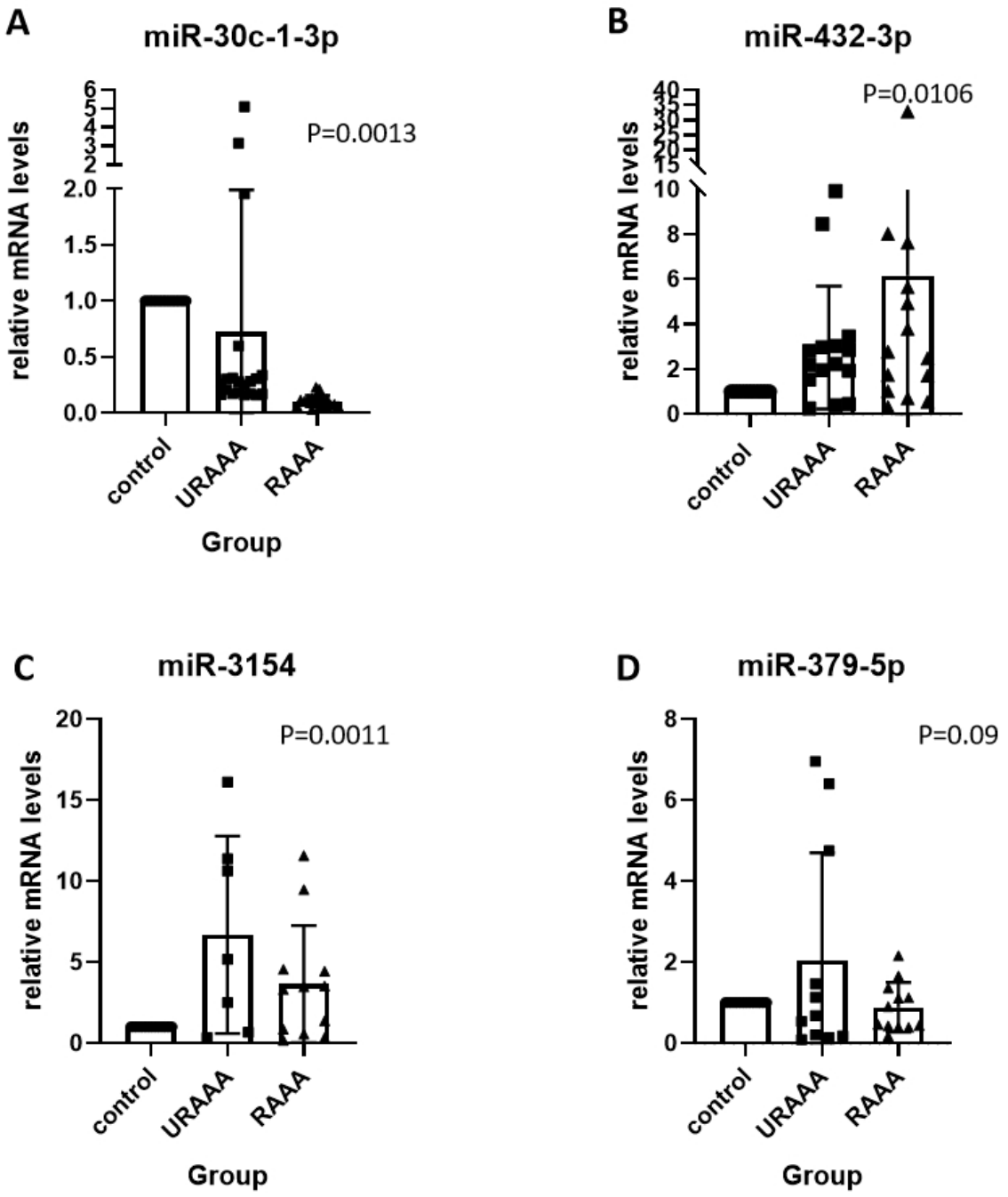

Figure 3

The results indicated that plasma levels of hsa-miR-30c-1-3p were significantly lower (P=0.0013), whereas those of hsa-miR-432-3p were significantly higher in the RAAA group than in the control and URAAA groups (P=0.0106) (Figure 3A, B). The expression of miR-3154 was the highest in the URAAA group, followed by the RAAA group and control group and that of miR-379-5p was the highest in the URAAA group, followed by the control group and URAAA group (Figure 3C, D).

Figure 4

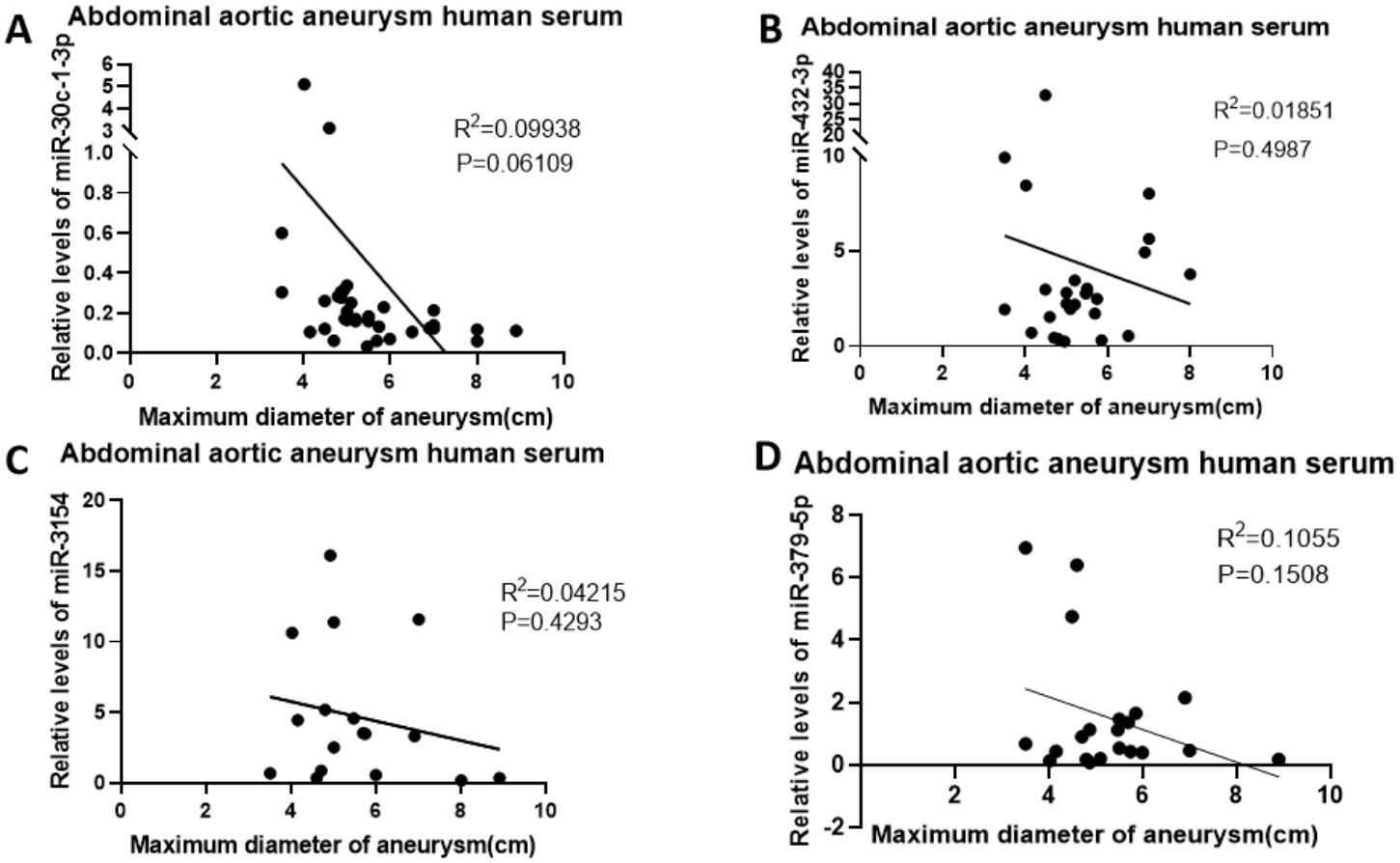

Figure 4

Bivariate correlation analysis showed that plasma levels of miR-30c-1-3p in patients with AAA tended to be negatively correlated with the maximal aortic diameter (Pearson correlation coefficient r = -0.3153, P = 0.06109) (Figure 4A). There was no correlation between plasma levels of mir-432-3p (Pearson correlation coefficient r = 0.01851, P = 0.4987), mir-3154 (Pearson correlation coefficient r = 0.04215, P = 0.4293), and mir-379-5p (Pearson correlation coefficient r = 0.1055, P = 0.1508) and the maximal aortic diameter in patients with AAA (Figure 4B–D).

Figure 5

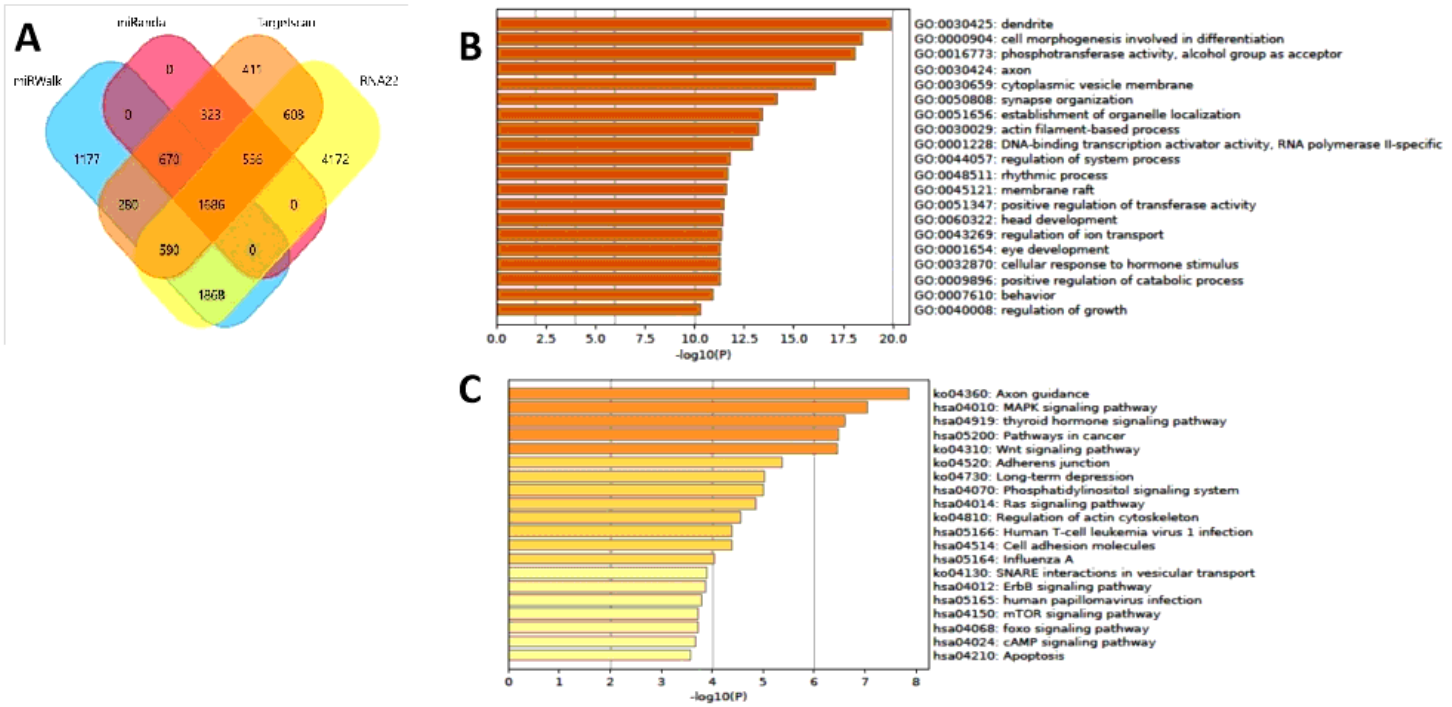

Figure 5

To disclose potential physiological mechanisms regulated by differentially expressed miR-30c-1-3p, its target genes were predicted using miRWalk, miRanda, RNA22, and Targetscan, and the common targets identified by the four databases were revealed by the Venn diagram (Figure 5A). Next, the target genes were functionally annotated using Gene Ontology (GO) and Kyoto Encyclopedia of Genes and Genomes (KEGG) databases. The target genes of miR-30c-1-3p were distributed according to GO biological processes, cell composition, and molecular function (Figure 5B). KEGG pathway analysis revealed the top three enriched pathways for miR-30c-1-3p targets, which were axon guidance, MAPK signaling pathway, and thyroid hormone signaling pathway (Figure 5B).

Figure 6

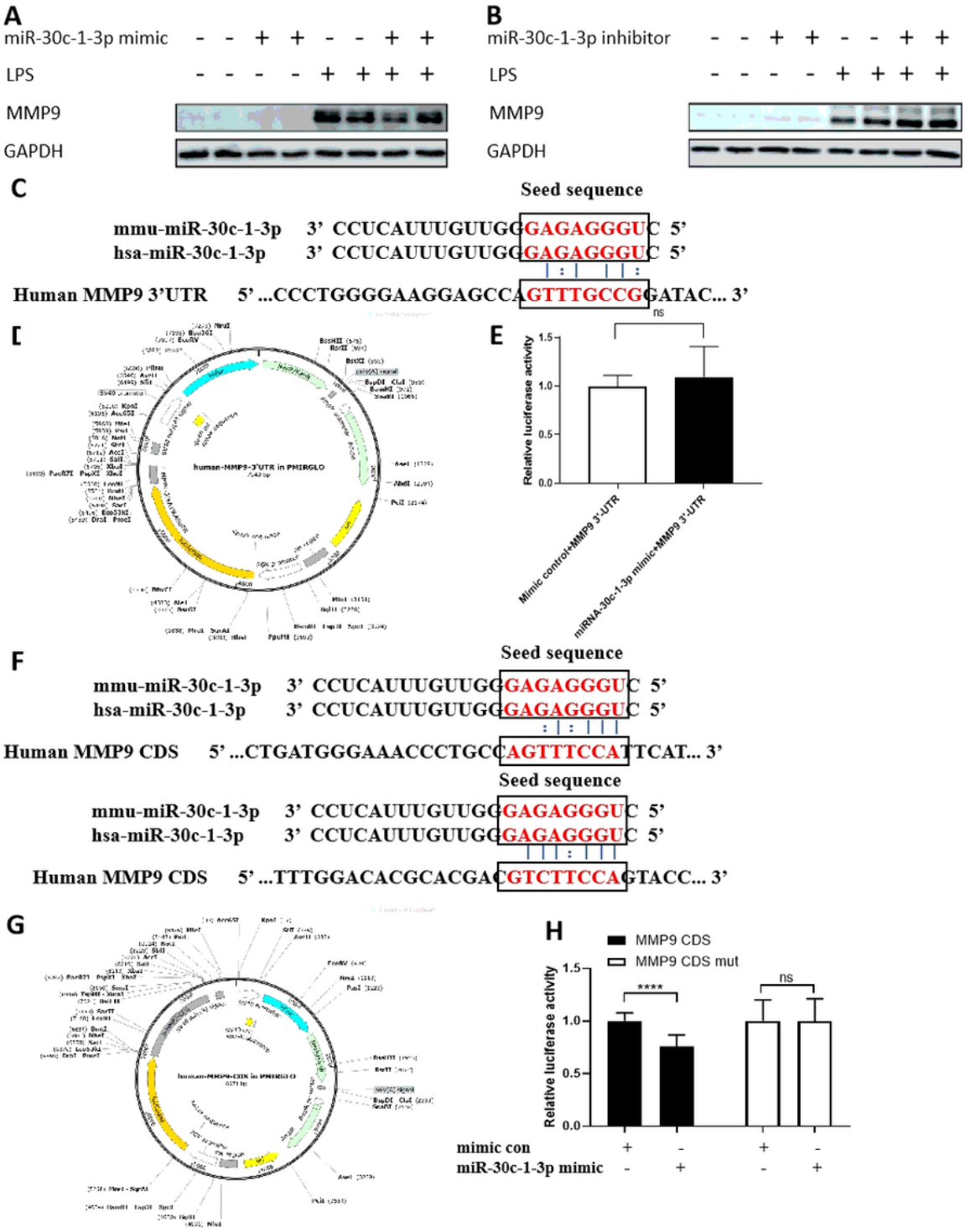

Figure 6

Western blot analysis showed that miR-30c-1-3p overexpression decreased the expression of MMP-9 in RAW264.7 cells, whereas its inhibition had the opposite effect (Figure 6A, B). To further examine the inhibitory effect of miR-30c-1-3p on MMP-9 expression, we transfected HEK293 cells with a reporter vector for the 3'-UTR of MMP-9, which contained miR-30c-1-3p-targeted base pairs (Figure 6C, D). However, the dual-luciferase reporter assay did not reveal significant differences in luciferase activity

between cells co-transfected with 3'-UTR and miR-30c-1-3p mimic or scrambled control (Figure 6E), indicating that miR-30c-1-3p did not regulate MMP-9 expression through its 3'-UTR. Interestingly, we found another conserved miR-30c-1-3p target site in the MMP-9 coding sequence (Figure 6F, G), and it appeared to be the region through which miR-30c-1-3p regulated MMP-9 expression according to the reporter assay (Figure 6H). To validate this result, we mutated the MMP-9 site targeted by miR-30c-1-3p in the coding sequence and co-transfected HEK293 cells with the mutated vector and miR-30c-1-3p or scrambled control. There was no significant difference in MMP-9 expression between the cells transfected with miR-30c-1-3p or control miR (Figure 6H), confirming that miR-30c-1-3p inhibited MMP-9 expression through binding to its coding sequence.

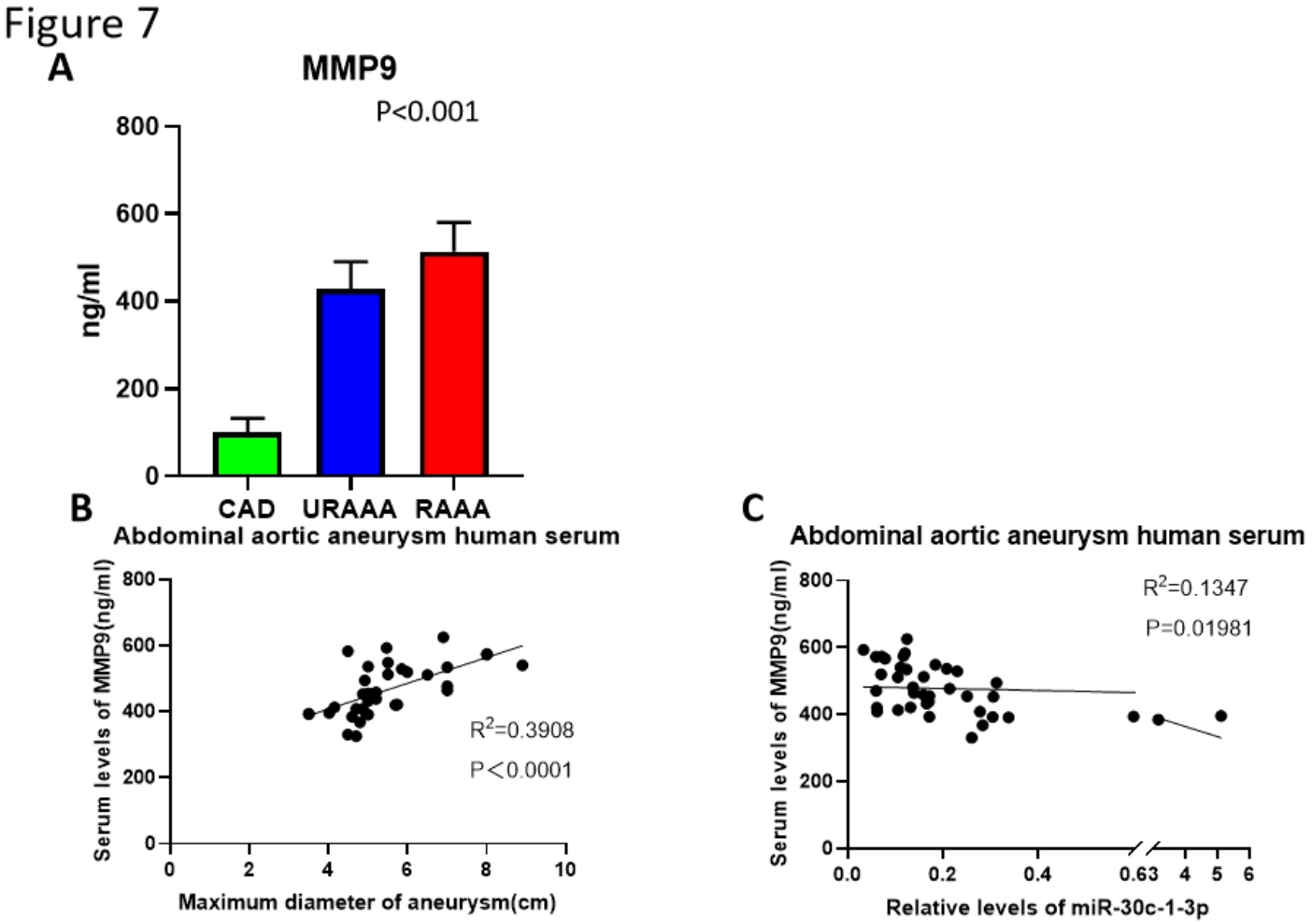

Figure 7

Analysis of patients' samples revealed that MMP-9 plasma concentration was increased in the URAAA and RAAA groups compared to control ($P < 0.001$) and in the RAAA group compared to the URAAA group ($P < 0.001$) (Figure 7A, Supplemental Table 2). Bivariate correlation analysis indicated that MMP-9 levels in plasma of patients with AAA was positively correlated with the maximal aortic diameter ($r = 0.6251$, $P < 0.0001$; Figure 7B) and negatively – with miR-30c-1-3p expression ($r = -0.3671$, $P = 0.01981$; Figure 7C).

Figure 8

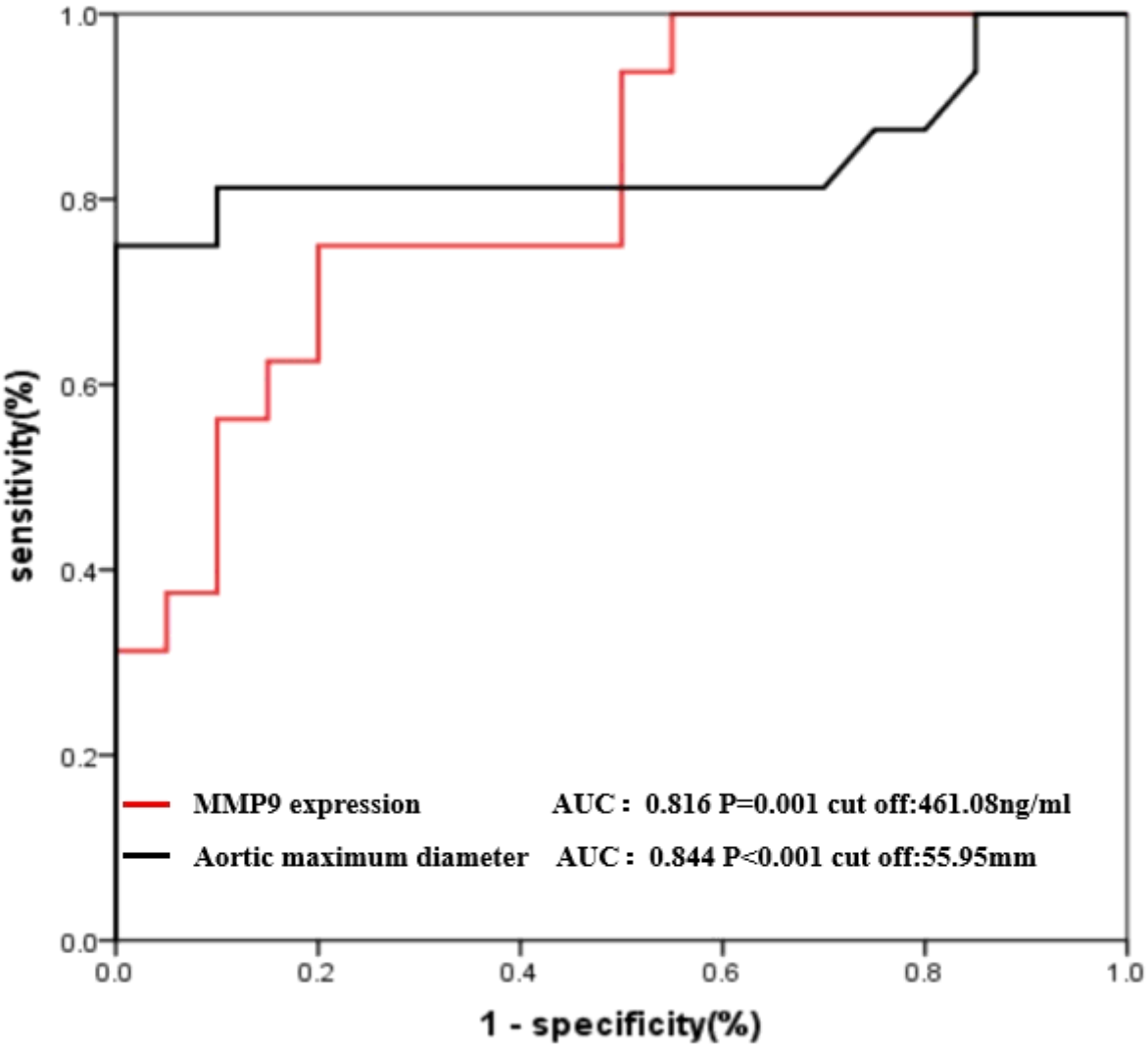

Figure 8

Receiver operating characteristic (ROC) curve analysis demonstrated that MMP-9 expression and the maximum aortic diameter could be used to distinguish patients with URAAA from those with RAAA (Figure 8). The optimal cutoff values for MMP-9 expression and the maximal aortic diameter were 461.08 ng/ml and 55.95 mm with areas under the curve of 0.816 and 0.844, respectively.

Supplementary Files

This is a list of supplementary files associated with this preprint. Click to download.

- SupplementalTable.doc